THE JOURNAL OF PHYSICAL CHEMISTRY A

 VOLUME 108, NUMBER 25, JUNE 24, 2004

LETTERS

Tracking Waves and Spiral Drift in Reaction−Diffusion Systems with Finite Bandwidth Dispersion Relations

Niklas Manz and Oliver Steinbock*

Department of Chemistry and Biochemistry, Florida State University, Tallahassee, Florida 32306-4390

Received: April 7, 2004; In Final Form: May 17, 2004

We report experimental results on chemical waves in 1,4-cyclohexanedione Belousov−Zhabotinsky systems that obey finite bandwidth dispersion relations. Although solitary pulses and long-wavelength pulse trains are unstable, pacemakers can generate short-wavelength patterns in which fast waves periodically annihilate at the slowly expanding pattern boundary. Along these boundaries, one finds numerous traveling defects that can nucleate rotating spirals which drift outward with the island's boundary. The drift follows logarithmic spirals and can induce spiral pair annihilation.

Many chemical and biological systems show propagating concentration waves that arise from diffusion-mediated spatial coupling of nonlinear reactions.[1] Examples include traveling waves in the CO oxidation on platinum surfaces,[2] the Belousov−Zhabotinsky (BZ) reaction,[3] and intracellular calcium waves in the cytosol of *Xenopus* oocytes[4] and cardiac myocyctes.[5] An important feature of these excitable media is the dispersion relation that describes the speed of wave trains, c, in terms of the period T or the wavelength λ. Several experimental studies of the classic BZ reaction revealed monotonically increasing dispersion relations.[6,7] They converge to a maximum value, c_0, for large wavelengths following a hyperbolic-tangent dependence[8] and have a short-wavelength limit below which no stable pulse trains exist.

Exceptions to this typical behavior are found in a modified BZ reaction that employs 1,4-cyclohexanedione (CHD) as its organic substrate. CHD−BZ systems have nonmonotonic dispersion relations that are characterized by a normal branch ($dc/d\lambda > 0$) for small wavelengths and an anomalous branch ($dc/d\lambda < 0$) for large wavelengths.[9−11] This anomaly gives rise to a variety of interesting phenomena such as "stacking" and "merging" waves. Both effects are observed in the wake of a wave front that propagates at a small velocity c_0 into the steady-state medium. Due to the anomalous shape of the dispersion curve, subsequent pulses are faster and either stack or vanish ("merge") as they approach the frontier pulse. Similar dynamics have been reported for experiments on the catalytic reduction of NO with CO on a Pt(100) surface.[12] Additional types of anomalous dispersion include dispersion curves with damped oscillations,[13] bistable domains,[14] and velocity gaps.[15]

Recently, we identified a type of dispersion relation that is qualitatively different from the cases mentioned above.[16] We showed that the dispersion curve in the CHD−BZ reaction can be limited to a finite band of wavelengths. Within this band the curve has normal slopes for short wavelengths and anomalous slopes for long wavelengths. In such systems, solitary pulses and finite wave trains are unstable. Nonetheless, periodic wave patterns can expand if the frequency of their pacemaker is sufficiently high. This unusual growth phenomenon involves the periodic annihilation of pulses at the pattern boundary. In this process, each pulse "clears the way" for its successor, which led us to coin the term "tracking waves" for these pulses. Here, we describe the first examples of tracking wave patterns in two-dimensional systems. In particular, we show that these dissipative structures can give rise to drifting and annihilating spiral waves.

The CHD−BZ reaction involves the oxidation of 1,4-cyclohexanedione by bromate in sulfuric acid solution. The

* To whom correspondence should be addressed. E-mail: steinbck@chem.fsu.edu

10.1021/jp048456g CCC: $27.50
Published on Web 05/29/2004

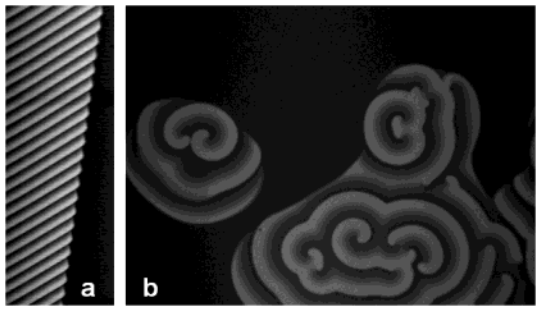

Figure 1. Tracking waves in the CHD−BZ reaction. (a) Space-time plot of a pseudo one-dimensional system. The vertical and horizontal axes span 600 s and 8.7 mm, respectively and time evolves in upward direction. (b) Snapshot of a pseudo two-dimensional system. Field of view: (14 × 21) mm^2. Initial concentrations in mol/L: [H_2SO_4] = 0.60 (a,b), [$NaBrO_3$] = 0.20 (a), 0.10 (b), [CHD] = 0.20 (a), 0.11 (b), and [catalyst] = 0.5×10^{-3} (a,b).

reaction solution is prepared in Nanopure water (18 MΩ cm) from stock solutions of $NaBrO_3$ (Fluka), 1,4-cyclohexanedione (Aldrich), sulfuric acid (Riedel-de Haën, 5 M), and $[Fe(batho(SO_3)_2)_3]^{4-}$ (Fluka and Acros, 25 mM). The iron catalyst also serves as redox indicator and allows the detection of wave patterns with a monochrome charge coupled device camera (COHU 2122). To create pseudo one- or pseudo two-dimensional systems, the reaction solution is filled into glass capillaries (inner diameter 0.8 mm) or into batch reactors in which the solution is confined between two planar polystyrene plates spaced at 0.4 mm. Spontaneous wave propagation commences after an induction time of approximately 80−90 min, during which the system remains in an unexcitable, oxidized state. In the pseudo one-dimensional case, waves typically nucleate at the open ends of the capillary where bromine escapes from the reaction medium into the ambient atmosphere. To achieve better control of wave nucleation in our two-dimensional systems, we carried out some experiments in which bromine leaves the reaction layer through a small hole in the upper plate. This is a simple and reliable way to create a pacemaker at a predetermined position, but in no way necessary for the phenomena described here. All experiments were carried out at room temperature.

Figure 1 shows tracking waves in CHD−BZ systems that obey finite bandwidth dispersion relations. Bright and dark areas correspond to oxidized and reduced regions, respectively. Figure 1a is a space−time plot of oxidation waves propagating in a one-dimensional system from the left to the right. The plot is generated by piling up subsequent absorption profiles. In this typical experiment, all waves are generated at left edge of the capillary tube with a period of $T = 26$ s. Each of the resulting wave pulses generates a bright band within the space−time plot. The rest state of the system is highly inhibited and does not allow stable propagation of wave pulses. Accordingly, all oxidation pulses vanish as they enter the reduced region on the right-hand side of the space−time plot. However, this annihilation process is not instantaneous, and each pulse advances slightly farther than its predecessor. For the given wave period and set of initial concentrations, the wave pattern grows $\Delta x = 148$ μm per pulse and, thus, expands with a constant speed of $\Delta x/T = 5.7$ μm/s.

The snapshot in Figure 1b shows an example of tracking waves in a two-dimensional system. The patterns are confined to small islands with rotating spirals as pacemakers. The wave fronts terminate as defects at the islands' boundaries. In the course of time, the islands grow with a constant speed as fronts vanish periodically at the boundary. In this respect, the behavior of two-dimensional systems is similar to the dynamics shown in Figure 1a. However, noncircular islands decrease the curvature of their boundary, and domains can fuse in inter-island collisions.

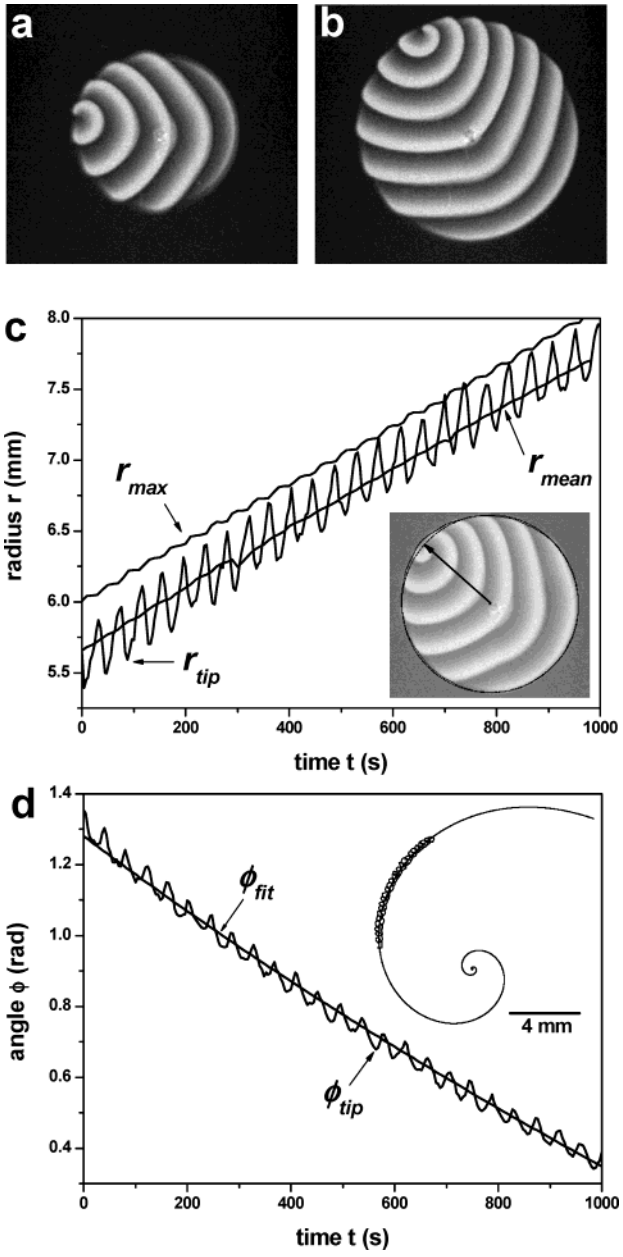

Figure 2. Spiral drift in an island of tracking waves. (a,b) Two snapshots with $\Delta t = 1100$ s. Field of view: (20 × 18) mm^2. (c) Maximal (r_{max}) and average (r_{mean}) radius of the wave island as a function of time along with the radial coordinate r_{tip} of the drifting spiral tip. The inset shows two black curves that are the boundary of the wave island and the corresponding best-fit circle. The curves are superimposed onto a snapshot of the pattern. The arrow points from the island's center to the spiral tip position. (d) Temporal evolution of the angular tip coordinate ϕ_{tip} and its best fit ϕ_{fit} based on eq 1a. The inset shows the tip trajectory and the best-fit logarithmic spiral in Cartesian coordinates. Initial concentrations as in Figure 1b.

In nearly all two-dimensional experiments, tracking wave patterns are organized by rotating spirals. These vortices nucleate primarily at the island's boundary from open-ended front segments. The transition from nonrotating defects to spiral waves seems to be triggered by small perturbations that alter the position of the defect with respect to its predecessor. After nucleation, the spiral core often remains stationary within the growing island. In other cases, however, the spiral tip drifts

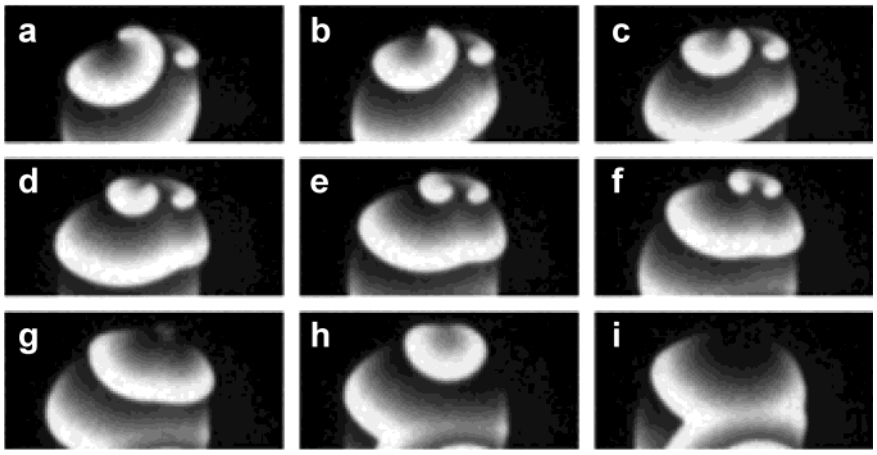

Figure 3. Sequence of nine consecutive snapshots of a spiral wave pair at the boundary of a tracking wave island. The spiral tips drift toward each other and annihilate. Field of view: (10 × 5) mm^2. Time between snapshots: 36 s. Initial concentrations as in Figure 1b.

along the boundary of the expanding wave island. A typical example of this phenomenon is shown in Figure 2. In panel a, the spiral wave is oriented in the nine o'clock direction at the boundary of a disk-shaped wave domain. This spiral is the only pacemaker within the island. The later snapshot in panel b reveals that this counterclockwise rotating vortex moves in clockwise direction along the island's edge. This drift lasts for approximately 25 rotation periods (∼1100 s) and ends in stationary spiral rotation.

We analyze the shape and the speed of the wave island by integrating the gray level intensity $I(x,y,t)$ over time intervals $[t - T/2, t + T/2]$ where T denotes the rotation period of the spiral (here $T = 45$ s). This procedure yields a sequence of frames in which the island is a homogeneously bright disk. From these data, we find that the island's center of mass is stationary and that its overall shape is nearly circular (see inset of Figure 2c). Close to the spiral tip, this circular shape is deformed by a convex bump that moves along with the tip in counterclockwise direction. Figure 2c shows the maximal and the average radius of the wave island as a function of time. Due to the small, spiral tip induced deformation, these two curves are on average offset by 330 μm. Both data sets indicate that the island grows with a constant speed of $v_i = (0.12 \pm 0.01)$ mm/min. The third curve in Figure 2c describes the temporal evolution of the distance of the spiral tip from the island's center. The average radial drift speed is $v_r = (0.13 \pm 0.01)$ mm/min and, hence, nearly identical to v_i. These values are approximately 30 times smaller than the wave speed. Further analysis reveals also that the drift velocity in the direction tangential to the island's boundary is constant. In polar coordinates (r, ϕ), this velocity is $v_\phi = r\,\dot{\phi}$ and a corresponding analysis yields $v_\phi = -(0.37 \pm 0.01)$ mm/min. Consequently, the spiral drift occurs in a direction that is characterized by a constant angle $\theta = \arctan(v_\phi/v_r) = -72°$ with respect to the normal vector of the island's boundary.

This result allows us to calculate the trajectory $(\phi(t), r(t))$ along which the average spiral drift occurs. Straightforward integration yields

$$\phi(t) = (v_\phi/v_r)\,\ln[(v_r\,t)/r_0 + 1] + \phi_0 \qquad (1a)$$

$$r(t) = v_r\,t + r_0 \qquad (1b)$$

where ϕ_0 and r_0 denote the polar coordinates of the spiral tip at time $t = 0$. Notice that eqs 1a and 1b describe a logarithmic spiral of the form $r(\phi) = r_0 \exp[v_r\,(\phi - \phi_0)/v_\phi]$. Figure 2d shows that the temporal evolution of the angular coordinate of the spiral tip is in good agreement with the theoretical curve computed from eq 1a and the parameters specified above. The inset of Figure 2d complements the result by showing the actual tip path in Cartesian coordinates along with the corresponding, extrapolated logarithmic spiral that describes its overall drift trajectory.

The drift of spiral tips along the expanding boundary of wave domains can give rise to the mutual annihilation of counter-rotating vortices. A typical example for this phenomenon is shown in Figure 3. In this experiment, two spirals are located at the upper boundary of a small wave island. The counterclockwise rotating spiral on the left occupies a slightly larger area than the clockwise spinning structure on the right. The first six snapshots (a−f) illustrate that the spiral tips undergo a drift that decreases their distance from approximately 2 mm to 0.4 mm. In the subsequent frames (g−i), the spiral pair vanishes after emitting a last circular wave front. The future fate of the island depends on the presence of additional wave sources. In particular, we observe that the entire island rapidly disappears if the colliding spirals are the only pacemakers.

In conclusion, we have shown that tracking waves in systems with finite bandwidth dispersion organize two-dimensional wave domains that expand with velocities significantly smaller than the typical pulse speed. Along the boundary of these islands, we find nonrotating defects that can nucleate rotating spiral waves. The resulting spirals are either stationary or drift with the island's boundary outward. Spiral drift occurs at a constant angle to the boundary and, hence, describes a logarithmic spiral. This type of vortex drift is unique in the sense that it involves neither externally imposed boundaries or gradients nor spiral-pair interaction (see e.g., refs 17−21). Nonetheless, it is useful to compare the drift directions in the latter studies with our findings. Markus et al. studied spiral waves in the photosensitive BZ reaction and found that the spiral tips move toward regions of higher light intensity and, hence, toward regions of higher inhibition, which might be related to the outward motion of drifting spirals in our experiments.[18] Zykov and Müller studied BZ spirals in small circular disks with impermeable walls and observed that counterclockwise rotating spirals drift in counterclockwise direction along the system boundary.[19] In our experiments, however, counterclockwise rotating spirals drift clockwise. This seeming discrepancy is caused by the unusual interface between the wave island and its surrounding medium, which is profoundly different from a simple impermeable wall. First, the interface itself moves outward and is of variable shape (cf., inset of Figure 2c). Second, it is likely that the tip rotation is affected by an inhibition gradient across the island/surround-

ings interface. This gradient could be the source of the observed drift trajectories that consist of low-curvature segments during rotation phases in which the tip is "unprotected" pointing into the inhibited surroundings and high-curvature segments during rotation phases in which the tip is "protected" by its own arm pointing into the island.

Acknowledgment. This work was supported by the National Science Foundation (NSF Grant CHE-20023105) and the Deutsche Akademie für Naturforscher Leopoldina (Grant BMBF-LPD 9901/8-85).

References and Notes

(1) Kapral, R.; Showalter, K., Eds. *Chemical Waves and Patterns*; Kluwer: Dordrecht, The Netherlands, 1995.
(2) Ertl, G.; Rotermund, H. H. *Curr. Opin. Solid State Mater*. **1996**, *1*, 617−621.
(3) Sagues, F.; Epstein, I. R. *Dalton Trans.* **2003**, *7*, 1201−1217.
(4) Fontanilla, R. A. et al. *Biophys. J.* **1998**, *75*, 2079−2087.
(5) Wussling, M. H. P.; Salz, H. *Biophys. J.* **1996**, *70*, 1144−1153.
(6) Sevcikova, H.; Marek, M. *Physica D* **1989**, *39*, 15−21.
(7) Steinbock, O.; Müller, S. C. *Physica A* **1992**, *188*, 61−67.
(8) Flesselles, J.-M.; Belmonte, A.; Gaspar, V. *J. Chem. Soc., Faraday Trans.* **1998**, *94*, 851−855.
(9) Hamik, C. T.; Manz, N.; Steinbock, O. *J. Phys. Chem. A* **2001**, *105*, 6144−6153.
(10) Hamik, C. T.; Steinbock, O. *Phys. Rev. E* **2002**, *65*, 046224.
(11) Hamik, C. T.; Steinbock, O. *New J. Phys.* **2003**, *5*, 1−12.
(12) Christoph, J.; Eiswirth, M.; Hartmann, N.; Imbihl, R.; Kevrekidis, I.; Bär, M. *Phys. Rev. Lett.* **1999**, *82*, 1586−1589.
(13) Winfree, A. T. *Physica D* **1991**, *49*, 125−140.
(14) Bordiougov, G.; Engel, H. *Phys. Rev. Lett.* **2003**, *90*, 148302.
(15) Falcke, M.; Or-Guil, M.; Bär, M. *Phys. Rev. Lett.* **2000**, *84*, 4753−4756.
(16) Manz, N.; Hamik, C. T.; Steinbock, O. *Phys. Rev. Lett.*, in press.
(17) Steinbock, O.; Schütze, J.; Müller, S. C. *Phys. Rev. Lett.* **1992**, *68*, 248−251.
(18) Markus, M.; Nagy-Ungvarai, Z.; Hess, B. *Science* **1992**, *257*, 225−227.
(19) Zykov, V. S.; Müller, S. C. *Physica D* **1996**, *97*, 322−332.
(20) Brandtstädter, H.; Braune, M.; Schebesch, I.; Engel, H. *Chem. Phys. Lett.* **2000**, *323*, 145−154.
(21) Sakurai, T.; Mihaliuk, E.; Chirila, F.; Showalter, K. *Science* **2002**, *296*, 2009− 2012.